

1 Ocean mediation of tropospheric response to reflecting and absorbing aerosols

2

3 Yangyang Xu^{1*} and Shang-Ping Xie²

4

5 ¹National Center for Atmospheric Research, Boulder, CO 80303.

6 ²Scripps Institution of Oceanography, University of California, San Diego, La Jolla, CA 92093.

7 *Correspondence to: yangyang@ucar.edu

8

9 ~~Revised for Atmospheric Chemistry and Physics~~

Yangyang 4/6/2015 1:01 PM

Deleted: Submitted to

10 ~~April 6, 2015~~

Yangyang 4/6/2015 1:01 PM

Deleted: Jan 24

11 ~~▲~~

Yangyang 4/6/2015 1:01 PM

Formatted: Font:12 pt

14 Abstract

15 Radiative forcing by reflecting (e.g., sulfate, SO₄) and absorbing (e.g., black carbon, BC)
16 aerosols is distinct: the former cools the planet by reducing solar radiation at the top of the
17 atmosphere and the surface, without largely affecting the atmospheric column, while the latter
18 heats the atmosphere directly. Despite the fundamental difference in forcing, here we show that
19 the structure of the tropospheric response is remarkably similar between the two types of
20 aerosols, featuring a deep vertical structure of temperature change (of opposite sign) in the
21 Northern Hemisphere (NH) mid-latitudes. The deep temperature structure is anchored by the
22 slow response of the ocean, as large meridional sea surface temperature (SST) gradient drives an
23 anomalous inter-hemispheric Hadley circulation in the tropics and induces atmospheric eddy
24 adjustments in the NH mid-latitudes. The tropospheric warming in response to projected future
25 decline in reflecting aerosols poses additional threats to the stability of mountain glaciers in NH.

26 Additionally, robust tropospheric response is unique to aerosol forcing and absent in the CO₂
27 response, which can be exploited for climate change attribution.

28 ▲

Yangyang 4/6/2015 1:01 PM

Deleted: The robust tropospheric response is unique to aerosol forcing and absent in the CO₂ response, which can be exploited for climate change attribution.

Yangyang 4/6/2015 1:01 PM

Formatted: Font: 12 pt

33 1. Introduction

34 Greenhouse gas-induced global warming is partially masked (Ramanathan and Feng, 2008) by
35 the accompanying increase in anthropogenic aerosols (Smith et al., 2011). Relative contribution
36 of aerosol masking effect on global temperature is hard to quantify for the following reasons: (a)
37 some aerosols (e.g., black carbon (BC) and organics) absorb sunlight and heat the planet (Bond
38 et al., 2013) and (b) aerosol microphysical effects on clouds are complex (Rosenfeld and Wood,
39 2013). Many ongoing efforts aim to reduce uncertainties in radiative forcing (Xu et al., 2013)
40 and quantify the surface temperature response to aerosols (Levy et al., 2013). The atmospheric
41 circulation response to reflecting aerosols has important effects on regional climate (e.g., the
42 Indian monsoon (Bollasina et al., 2011)) and hydrological cycle (Shindell et al., 2012; Hwang et
43 al., 2013). Much attention has been given to absorbing aerosols for the direct atmospheric
44 heating effect, including BC (Meehl et al., 2010) and dust (Vinoj et al., 2014). It is often argued
45 that, by heating directly the atmosphere, absorbing aerosols can greatly perturb the atmospheric
46 temperature structure, causing changes in stability and circulation (Lau et al., 2006). The
47 atmospheric response, especially that of clouds, is hypothesized to be sensitive to the vertical
48 profile of atmospheric heating (Koch and Del Genio, 2010). Reflecting aerosols, however, are
49 hinted less effective in driving large-scale circulation changes (Allen et al, 2012).

50 While previous studies (e.g. Xie et al., 2013; Ocko et al., 2014) focused on radiative forcing and
51 climate impacts of aerosols on surface temperature and precipitation (Table S1), few looked at
52 the tropospheric response. Using climate model simulations, we show that the atmospheric
53 responses (temperature and circulation) to reflecting and absorbing aerosols are surprisingly
54 similar in structure (aside from a sign difference). Both responses feature a deep vertical

Yangyang 4/6/2015 1:01 PM

Deleted: dusts

Yangyang 4/6/2015 1:01 PM

Deleted: considered

57 | temperature structure in the Northern Hemisphere (NH) mid-latitudes, with a meridional shift in
58 | the westerly jet. Such a strong atmospheric temperature response to absorbing aerosols has been
59 | commonly linked to direct solar absorption in the atmosphere (Lau et al., 2006). We
60 | demonstrate, however, that changes in the sea surface temperature (SST) gradient and mid-
61 | latitude eddies are instrumental in creating a common deep vertical temperature in response to
62 | both types of aerosols, despite the fundamental difference in their forcing structure.

63 | 2. Methods

64 | 2.1 The global climate model

65 | CESM1 (Community Earth System Model 1) is a coupled ocean–atmosphere–land–sea-ice
66 | model. CESM1 climate projections for the 21st century have been documented extensively
67 | (Meehl et al., 2013). The anthropogenic forcings in CESM1 include long-lived greenhouse gases
68 | (GHGs), as well as tropospheric ozone, stratospheric ozone, sulfate aerosols, and black and
69 | primary organic carbon aerosols. The three-mode aerosol scheme (MAM3) provides internally
70 | mixed representations of aerosol number concentrations and masses (Liu et al., 2012). Aerosol
71 | indirect forcing is included for both liquid and ice phase clouds (Gettelman et al., 2010).

72 | The aerosol emission inventory is from the standard Representative Concentration Pathway as
73 | described in Lamarque et al. (2010). However, the present-day emission level of BC is adjusted
74 | from the standard model emission inventory to account for the potential model underestimation
75 | of BC atmospheric heating. Our previous analysis (Xu et al., 2013) show that such a correction
76 | improves simulated radiative forcing, compared to the direct observations. Without the
77 | observational constrains, simulated BC forcing (and associated temperature response) would be

- Yangyang 4/6/2015 1:01 PM
Deleted: similar
- Yangyang 4/6/2015 1:01 PM
Deleted: simulations
- Yangyang 4/6/2015 1:01 PM
Deleted: forcing
- Yangyang 4/6/2015 1:01 PM
Deleted: prescribed time- and space-evolving concentrations of
- Yangyang 4/6/2015 1:01 PM
Deleted: the direct effect of
- Yangyang 4/6/2015 1:01 PM
Deleted: (Lamarque et al
- Yangyang 4/6/2015 1:01 PM
Moved down [1]: ., 2010).
- Yangyang 4/6/2015 1:01 PM
Deleted: modal
- Yangyang 4/6/2015 1:01 PM
Deleted: has been implemented, and it
- Yangyang 4/6/2015 1:01 PM
Deleted: a
- Yangyang 4/6/2015 1:01 PM
Deleted: of
- Yangyang 4/6/2015 1:01 PM
Deleted: . Indirect
- Yangyang 4/6/2015 1:01 PM
Deleted: due to aerosols
- Yangyang 4/6/2015 1:01 PM
Moved (insertion) [1]
- Yangyang 4/6/2015 1:01 PM
Deleted: this model. The
- Yangyang 4/6/2015 1:01 PM
Deleted: forcing.
- Yangyang 4/6/2015 1:01 PM
Deleted: analyses
- Yangyang 4/6/2015 1:01 PM
Deleted: would improve model-
- Yangyang 4/6/2015 1:01 PM
Deleted: ,
- Yangyang 4/6/2015 1:01 PM
Deleted: with
- Yangyang 4/6/2015 1:01 PM
Deleted: observationally constrained values, the modeled
- Yangyang 4/6/2015 1:01 PM
Deleted: simulated
- Yangyang 4/6/2015 1:01 PM
Deleted: change

102 lower by about a factor of two. In addition to the atmospheric heating, deposition of BC particles
103 onto snow surface with high albedo would reduce surface albedo and contribute to surface
104 warming (Huang et al., 2011). The land model of CESM incorporates SNICAR (Snow and Ice
105 Aerosol Radiation) module, which represents the effect of aerosol deposition (BC, organic
106 carbon and dust) on surface albedo (Flanner et al., 2007).

Yangyang 4/6/2015 1:01 PM

Formatted: English (UK)

107 Note that in this study we used BC, a strong absorber, to characterize absorbing aerosols that also
108 include dust and organic aerosols. Similarly, we used SO4 to characterize reflecting aerosols
109 although dust and organic aerosols are also partially reflecting. This approach provided a clearer
110 contrast between these two types of aerosol forcing.

111 2.2 Model experiments

112 (a) Fully coupled model simulations with instantaneous forcing. We used a 394-year, pre-
113 industrial simulation as the control case. Starting from the end of the 319th year, we ran the
114 simulations for 75 years, with the last 60 years of output analyzed. This allows the first 15 years
115 for model spin-up to establish a quasi-equilibration with changes in radiative forcing (Long et al.
116 2014). The forcing is imposed by increasing BC emissions (as a proxy for absorbing aerosols)
117 and SO2 emissions (a precursor of SO4, as a proxy for reflecting aerosols) instantaneously from
118 pre-industrial levels to the present-day level. This methodology is similar to the classical CO2
119 doubling experiment (Manabe and Wetherald, 1975). The long averaging time (60 years in the
120 perturbed simulation versus 394 years for the pre-industrial control simulations) enabled us to
121 dampen the influence of decadal natural variability and to obtain a clear effect due to aerosol
122 perturbation. To increase the signal-to-noise ratio in the BC case (due to a smaller BC forcing),
123 five ensembles of perturbed simulations were conducted.

Yangyang 4/6/2015 1:01 PM

Deleted: :

Yangyang 4/6/2015 1:01 PM

Deleted: , allowing

Yangyang 4/6/2015 1:01 PM

Deleted: .

127 (b) The 20th century transient simulations using fully coupled model, with time-evolving sulfate
128 forcing. The details of the simulations can be found in Meehl et al. (2013). The resolution of both
129 atmosphere and ocean models is 1 degree by 1 degree for the coupled simulations (Experiments
130 a and b) in this study.

Yangyang 4/6/2015 1:01 PM
Deleted: simulations
Yangyang 4/6/2015 1:01 PM
Deleted: .
Yangyang 4/6/2015 1:01 PM
Deleted:)

131 (c) The atmospheric-only simulations, with instantaneous forcing. The model setting and imposed
132 forcing are identical to (a), but SST is fixed at a pre-industrial level, with only seasonal
133 variability. The model was also run for 75 years.

Yangyang 4/6/2015 1:01 PM
Deleted: : the

134 (d) The SST perturbation experiment, The SST was perturbed according to the zonal mean of the
135 CESM SO4 Experiment a (Fig S1). This corresponds to with a temperature profile that varies
136 from 0 °C at 90°S to -0.5 °C at the equator, and then to -1.2 °C at 90°N. The SST perturbation
137 did not include any longitudinally varying pattern, as our focus here was to understand the zonal
138 averaged temperature response. The perturbed model was run for 25 years (with 10 years of daily
139 output, for eddy flux analysis). The resolution of atmospheric model is 2 degree by 2 degree for
140 the uncoupled simulations (Experiments c and d) in this study.

Yangyang 4/6/2015 1:01 PM
Deleted: : the
Yangyang 4/6/2015 1:01 PM
Deleted: gradient
Yangyang 4/6/2015 1:01 PM
Deleted: increased linearly with latitude,
Yangyang 4/6/2015 1:01 PM
Deleted: K
Yangyang 4/6/2015 1:01 PM
Deleted: K
Yangyang 4/6/2015 1:01 PM
Deleted: K

141 3. Tropospheric response linked to SST gradient

Yangyang 4/6/2015 1:01 PM
Deleted: The values were determined by calculating the SST response to SO4 in experiment (a).

142 BC atmospheric radiative forcing is concentrated at 30°N and extends well above the boundary
143 layer to the free atmosphere (Fig. 1), a structure determined by atmospheric concentration, and
144 indirectly by emission sources. Intuitively, solar absorption by BC results in atmospheric
145 warming. Indeed, BC (Fig. 1 upper panels) induces a warming maximum in the NH mid-latitude
146 troposphere (350 mb, 30 to 40°N) in the coupled ocean-atmosphere model, which dwarfs the
147 upper tropical and Arctic warming. This simple thermodynamic mechanism seems consistent

Yangyang 4/6/2015 1:01 PM
Deleted:).
Yangyang 4/6/2015 1:01 PM
Deleted: 3. Results and discussions -

Yangyang 4/6/2015 1:01 PM
Deleted: S1
Yangyang 4/6/2015 1:01 PM
Deleted: emission sources and
Yangyang 4/6/2015 1:01 PM
Deleted: .
Yangyang 4/6/2015 1:01 PM
Deleted: 1 and Fig. S1 for annual mean
Yangyang 4/6/2015 1:01 PM
Deleted:),

168 with the fact that the magnitude of BC warming is much larger in the boreal summer (JJA) than
169 in the boreal winter (DJF) (Fig. 2 upper panels) due to solar insolation.

170 Interestingly, SO₄ also induces a similar enhanced tropospheric cooling in the mid-latitudes (Fig.
171 1 and Fig. 2). For easy comparison, the response is reversed in sign to be positive. The deep
172 atmospheric response is unexpected from the weak, direct atmospheric forcing of reflecting
173 aerosols (Fig. 1 middle left). Also contradictory to the above thermodynamic argument for BC,
174 the temperature response to SO₄ is of a similar magnitude in DJF and JJA (Fig. 2). The CO₂
175 response features a structure of amplified upper tropical troposphere warming (maximum at
176 around 300 mb), which is a robust feature due to thermodynamical adjustment of the tropical
177 atmosphere to maintain a moist adiabatic lapse rate there. The lower tropospheric atmospheric
178 temperature over the Arctic also has a larger response, mostly due to stronger snow albedo
179 feedback.

180 The climate response may be decomposed into fast and slow components, defined as the
181 atmospheric response without and due to SST change, respectively (Ganguly et al., 2012). The
182 BC temperature response results predominately from the fast component in the summer due to
183 direct atmospheric heating (Fig. 3), but the slow response dominates in the winter. The SO₄ fast
184 response, due to the lack of atmospheric forcing, is strikingly small (except in summer polar
185 regions where air temperature above sea ice is free to change), despite aerosol indirect forcing
186 through fast adjustment of clouds are allowed. The SO₄ slow response in winter features a
187 narrow maximum around 30°N, and the summer mid-latitude response is weaker and extends
188 into the upper tropics. Therefore, the slow component of the response due to SST change is

Yangyang 4/6/2015 1:01 PM

Deleted: 1st row in

Yangyang 4/6/2015 1:01 PM

Deleted: 1

Yangyang 4/6/2015 1:01 PM

Deleted: S1 for annual mean).

Yangyang 4/6/2015 1:01 PM

Deleted: S1

Yangyang 4/6/2015 1:01 PM

Deleted: 2

Yangyang 4/6/2015 1:01 PM

Deleted: negligible during summer

Yangyang 4/6/2015 1:01 PM

Deleted:).

196 entirely responsible for the SO4 deep atmospheric response and partially responsible for the BC
197 response.

198 The dominant role of SST in causing the deep atmospheric response is further confirmed by a set
199 of perturbed-SST experiments, in which the zonal mean SST change in the full SO4 simulation
200 (Fig. S1) is applied to the atmospheric-only model, but with no radiative forcing. The model
201 response to the perturbed SST (3rd row of Fig. 2) is remarkably similar to the SO4 slow response
202 (Fig. 3), explaining a large fraction of the total response (2nd row of Fig. 2). The boundary layer
203 air temperature (below 850 mb) is closely tied to the underlying SST because of turbulent
204 mixing, while in the mid-latitudes, the free atmospheric temperature is not tied to the SST
205 because the atmosphere is stably stratified. However, changes in the SST may affect the free
206 troposphere through ~~the changes of tropical circulations and mid-latitude eddy, which we explore~~
207 ~~next.~~

208 4. Understanding zonal mean circulation changes

209 Fig. 4 shows the circulation responses to aerosols in terms of meridional overturning stream
210 function (positive values indicate clockwise circulation) and zonal averaged zonal wind (positive
211 values indicate westerly winds). Note that the responses of SO4 and BC are similar in space but
212 of opposite signs. SO4 cooling in the NH induces an anomalous Hadley cell that rises in the SH
213 and sinks in the NH (also shown in Ocko et al., (2014)). The atmospheric model forced by SO4-
214 induced SST change largely reproduces the Hadley cell response (Fig. 4, bottom left),
215 highlighting the importance of the inter-hemispheric SST gradient. Consistent with the Hadley
216 cell response, the NH jet stream shifts equatorward in response to SO4, and vice versa to BC.
217 Following the thermal wind relationship (the maximum temperature gradient sets the maximum

Yangyang 4/6/2015 1:01 PM

Deleted: (Fig. 2).

Yangyang 4/6/2015 1:01 PM

Deleted: 1

Yangyang 4/6/2015 1:01 PM

Deleted: 2

Yangyang 4/6/2015 1:01 PM

Deleted: 1

Yangyang 4/6/2015 1:01 PM

Deleted: circulation and eddy adjustments

Yangyang 4/6/2015 1:01 PM

Deleted: The

Yangyang 4/6/2015 1:01 PM

Moved (insertion) [2]

Yangyang 4/6/2015 1:01 PM

Deleted: are shown

Yangyang 4/6/2015 1:01 PM

Deleted: the

Yangyang 4/6/2015 1:01 PM

Deleted: Fig. 3,

Yangyang 4/6/2015 1:01 PM

Moved up [2]: Fig.

Yangyang 4/6/2015 1:01 PM

Deleted: S3,

Yangyang 4/6/2015 1:01 PM

Deleted: response

Yangyang 4/6/2015 1:01 PM

Deleted: ,

Yangyang 4/6/2015 1:01 PM

Deleted: have

Yangyang 4/6/2015 1:01 PM

Deleted:).

Yangyang 4/6/2015 1:01 PM

Deleted: with

Yangyang 4/6/2015 1:01 PM

Deleted: 3rd row of

Yangyang 4/6/2015 1:01 PM

Deleted: 3

Yangyang 4/6/2015 1:01 PM

Deleted: (Fig. S3).
Stationary

238 zonal wind), the equatorward shift of westerly winds must be accompanied by a deep cooling
239 structure (Fig. 1 and Fig. 2).

240 The color scale for the SO₄ response in Fig. 4 is not reversed as in previous temperature figures,
241 in order to depict the real direction of circulation change. The magnitude of changes in response
242 to BC is weaker due to a smaller forcing magnitude (Table S1). In addition, the SO₄-induced
243 Hadley cell change is interhemispheric across the equator while the BC-induced Hadley cell
244 change appears more confined to the NH. The same for the jet stream shift. This is probably
245 because of the geographic difference in BC and SO₄ forcing (amid both are stronger in NH than
246 SH), which may influence the Pacific and Atlantic branches of jets differently.

247 Eddy fluxes that transport heat and momentum in meridional directions are instrumental in
248 maintaining the climatological mid-latitude jets. Here we use the Eliassen-Palm (EP) flux to
249 diagnose how eddy flux adjustment in response to aerosols leads to changes of zonal winds. The
250 EP flux vector, with its vertical component depicting the meridional heat flux and its meridional
251 component depicting the equatorward meridional momentum flux, is calculated using 10-year
252 daily data from the control and the perturbed SO₄ SST simulations following Holton (2004).

253 The NH annual mean EP flux and its divergence (in contour) are shown in Fig. 5a. Over
254 extratropical atmosphere, EP flux convergence (negative value) suggests that meridional heat
255 eddy flux (the vertical component of EP flux) acts to slow the westerly wind aloft (Holton,
256 2004). However, the strong equatorward wave propagation in the mid-latitude troposphere
257 (meridional component of EP flux) is acting to extract momentum from the tropics to the mid-
258 latitude, therefore maintaining the westerly wind at 40-60°N.

Yangyang 4/6/2015 1:01 PM

Deleted: Stationary

Yangyang 4/6/2015 1:01 PM

Deleted: activities (Fig. S4b)

261 Under the SO₄-induced SST perturbation, the EP flux change is found strongest in the NH mid-
262 latitudes 30-40°N, equatorward side of its climatology (Fig. 5b). Poleward EP flux anomalies
263 reduce the climatological equatorward wave propagation. In the middle troposphere (400-800
264 mb), EP flux convergence (blue) decelerates the vertically average westerly wind at 50-60°N,
265 while EP flux divergence (red) tends to accelerate the westerly wind at 30-40°N. Therefore,
266 westerly winds shift equatorward in response to SO₄ (Fig. 4). Of the total eddy flux, stationary
267 eddies contribute about 60% (Fig. 5c) with the rest coming from transient eddies. The EP flux
268 change occurs predominately during the NH winter, because the background mid-latitude wave
269 activity is stronger. This is shown by the larger vectors in Fig. 5d and stronger EP flux
270 divergence (red) at 30-40°N.

271 The change in EP flux is consistent with that in the stationary wave refractive index as wave
272 propagation is mainly from a high refractive index region to a low refractive index region (Held
273 and Hou, 1980; Fig. S2). The quasi-geostrophic refractive index and its change under SST
274 perturbation were calculated following Limpasuvan and Hartmann (2000). In the climatology
275 (Fig. S2a), the high refractive index is located in the mid and high latitudes, and the tropics are
276 mainly occupied by a smaller refractive index, facilitating the equatorward propagation of mid-
277 latitude wave activities (Fig. 5a, also seen in Sun et al., 2013). The refractive index negative
278 anomaly due to perturbed SO₄ SST is mainly found in the NH mid-latitude regions (Fig. S2b),
279 which causes the reduction of wave propagation to the equator (Fig. 5b).

280 The above diagnosis explains the SO₄ induced deep tropospheric cooling and associated
281 equatorward shift of westerly jet in the NH mid-latitudes. Firstly, the intensified NH Hadley cell
282 accelerates the upper tropospheric westerly jets in the subtropics. Secondly, the EP flux

Yangyang 4/6/2015 1:01 PM
Deleted: of the EP flux change in the NH,

Yangyang 4/6/2015 1:01 PM
Deleted: (about three times larger than the summer change, Fig. S4c) when

Yangyang 4/6/2015 1:01 PM
Deleted: strong (Sun et al., 2013).

Yangyang 4/6/2015 1:01 PM
Deleted: S5).

Yangyang 4/6/2015 1:01 PM
Deleted: S5a

Yangyang 4/6/2015 1:01 PM
Deleted:) (Fig S4a

Yangyang 4/6/2015 1:01 PM
Deleted: at

Yangyang 4/6/2015 1:01 PM
Deleted: Figure S5b

Yangyang 4/6/2015 1:01 PM
Deleted: then

Yangyang 4/6/2015 1:01 PM
Deleted: 4

Yangyang 4/6/2015 1:01 PM
Deleted: the

Yangyang 4/6/2015 1:01 PM
Deleted: : (1)

Yangyang 4/6/2015 1:01 PM
Deleted: westerlies

Yangyang 4/6/2015 1:01 PM
Deleted: ; (2)

298 divergence accelerates the westerly jet on the equatorward flank of the mean Hadley cell, while
299 the jet is decelerated on the poleward flank due to EP flux convergence. Both the Hadley and
300 eddy adjustments are anchored by the SST change with strong meridional gradients. Aqua-planet
301 model experiments exploring the response to an idealized mid-latitude heating (Ceppi et al.,
302 2013) supported our arguments here about the coupled adjustments of the Hadley circulation and
303 mid-latitude jets to realistic aerosol forcing.

- Yangyang 4/6/2015 1:01 PM
Deleted: (convergence)
- Yangyang 4/6/2015 1:01 PM
Deleted: (decelerates)
- Yangyang 4/6/2015 1:01 PM
Deleted: (
- Yangyang 4/6/2015 1:01 PM
Deleted:)
- Yangyang 4/6/2015 1:01 PM
Deleted: Idealized aqua
- Yangyang 4/6/2015 1:01 PM
Deleted: (Ceppi et al., 2013)
- Yangyang 4/6/2015 1:01 PM
Deleted: a simple
- Yangyang 4/6/2015 1:01 PM
Deleted: support
- Yangyang 4/6/2015 1:01 PM
Deleted: 4

304 5. Conclusions

305 Our results show that despite the fundamental difference in forcing structure, BC and SO4 share
306 common atmospheric response patterns. The common response is mediated by the ocean through
307 sea-surface temperature gradient, and insensitive to microphysical representations of aerosols.
308 This highlights the importance of ocean-atmosphere interactions in shaping large-scale patterns
309 of climate response (Xie et al. 2010), a process overlooked so far in aerosol-climate connection.

- Yangyang 4/6/2015 1:01 PM
Deleted: ,

310 The deep mid-latitude warming in response to BC contributes to the retreat of mountain glaciers
311 in the NH near anthropogenic BC emissions, including the Alps (Painter et al, 2013) and the
312 Himalayas. Although the cooling effect on the free troposphere is rarely discussed, SO4 aerosols
313 may have mitigated glacier retreats elsewhere in the past. Into the future, declining SO4 aerosols
314 may lead to an elevated atmospheric warming and pose a threat to mountain snow packs. This
315 implies that more stringent controls on BC and GHGs are needed to mitigate the snow pack
316 retreat.

- Yangyang 4/6/2015 1:01 PM
Formatted: Font:Not Italic
- Yangyang 4/6/2015 1:01 PM
Deleted: ,
- Yangyang 4/6/2015 1:01 PM
Formatted: Not Superscript/ Subscript
- Yangyang 4/6/2015 1:01 PM
Deleted: however, more stringent air pollution controls would result in a deep mid-latitude
- Yangyang 4/6/2015 1:01 PM
Deleted: , posing

317 The tropospheric temperature and circulation response to SO4 is also found in the 20th century
318 transient simulation (Fig. S3) and the 21st century multi-model projections (Rotstayn et al.,

- Yangyang 4/6/2015 1:01 PM
Deleted: seen
- Yangyang 4/6/2015 1:01 PM
Deleted: S2

336 2014). This suggests that the deep temperature structure in the mid-latitudes is a robust feature of
337 aerosol-induced climate change, probably insensitive to model sub-grid physics. The dynamic
338 response involving the inter-hemispheric Hadley circulation is weak in the case of CO₂ and
339 presumably other hemispherically symmetrical forcing (such as solar and volcanic activities).
340 The importance of SST pattern has been noted previously (Ramanathan et al., 2005; Xu and
341 Ramanathan, 2010; Friedman et al., 2013; Xie et al., 2013), and our study reveals a fundamental
342 difference in the mid-latitude atmospheric responses to CO₂ and aerosol forcing. This difference
343 can be exploited to improve the detection and attribution of climate change (Lu et al., 2008;
344 Santer et al., 2013). Because aerosol forcing involves stronger mid-latitude storm track
345 adjustments, our result also has implications for the attribution and projection of extreme events,
346 (e.g. blockings).

Yangyang 4/6/2015 1:01 PM

Deleted: (Fig. S1)

Yangyang 4/6/2015 1:01 PM

Deleted: generally for

Yangyang 4/6/2015 1:01 PM

Deleted: effects have

Yangyang 4/6/2015 1:01 PM

Deleted: but

Yangyang 4/6/2015 1:01 PM

Deleted: this

Yangyang 4/6/2015 1:01 PM

Deleted: important

Yangyang 4/6/2015 1:01 PM

Deleted: .

Yangyang 4/6/2015 1:01 PM

Formatted: Font:12 pt

355 Acknowledgments:

356 | The authors wish to thank Isaac Held, Paulo Ceppi, and Lantao Sun for discussions, and Joe
357 | Barsugli for sharing codes for EP flux. Y.X. is supported by the Regional and Global Climate
358 | Modeling Program (RGCM) of the U.S. Department of Energy's Office of Science (BER, DE-
359 | FC02-97ER62402) and the National Center for Atmospheric Research (NCAR) Advanced Study
360 | Programme (ASP) postdoctoral fellowship; and S.P.X. by the National Science Foundation
361 | (NSF). NCAR is funded by the NSF.

362 |

Yangyang 4/6/2015 1:01 PM
Formatted: Font:12 pt
Yangyang 4/6/2015 1:01 PM
Formatted: Line spacing: double

363 References:

364 Allen, R. J., Sherwood, S. C., Norris, J. R., and Zender, C. S.: Recent Northern Hemisphere
365 tropical expansion primarily driven by black carbon and tropospheric ozone. Nature, 485, 350–
366 354, 2012.

367 Bollasina, M. A., Ming, Y., and Ramaswamy, V.: Anthropogenic aerosols and the weakening of
368 the South Asian summer monsoon. Science, 334, 502–505, 2011.

369 Bond, T. C., Doherty, S. J., Fahey, D. W., Forster, P. M., Berntsen, T., Deangelo, B. J., Flanner,
370 M. G., Ghan, S., Kärcher, B., Koch, D., Kinne, S., Kondo, Y., Quinn, P. K., Sarofim, M. C., 5
371 Schultz, M. G., Schulz, M., Venkataraman, C., Zhang, H., Zhang, S., Bellouin, N., Guttikunda,
372 S. K., Hopke, P. K., Jacobson, M. Z., Kaiser, J. W., Klimont, Z., Lohmann, U., Schwarz, J. P.,
373 Shindell, D., Storelvmo, T., Warren, S. G., and Zender, C. S.: Bounding the role of black carbon
374 in the climate system: A scientific assessment. J. Geophys. Res. Atmos., 118, 5380– 5552, 2013.

375 Ceppi, P., Hwang, Y.-T., Liu, X., Frierson, D. M. W., and Hartmann, D. L.: The relationship
376 between the ITCZ and the Southern Hemispheric eddy-driven jet. J. Geophys. Res.-Atmos., 118,
377 5136–5146, 2013.

378 Flanner, M. G., Zender, C. S., Randerson, J. T. and Rasch, P. J.: Present-day climate forcing and
379 response from black carbon in snow, J. Geophys. Res. Atmos., 112(D11), D11202,
380 doi:10.1029/2006JD008003, 2007.

Yangyang 4/6/2015 1:01 PM

Deleted: . &

Yangyang 4/6/2015 1:01 PM

Deleted: .

Yangyang 4/6/2015 1:01 PM

Deleted: .

Yangyang 4/6/2015 1:01 PM

Deleted: 4

Yangyang 4/6/2015 1:01 PM

Deleted: a,

Yangyang 4/6/2015 1:01 PM

Deleted: . &

Yangyang 4/6/2015 1:01 PM

Deleted: .

Yangyang 4/6/2015 1:01 PM

Deleted: .

Yangyang 4/6/2015 1:01 PM

Deleted: 5

Yangyang 4/6/2015 1:01 PM

Deleted: . et al.

Yangyang 4/6/2015 1:01 PM

Deleted: .

Yangyang 4/6/2015 1:01 PM

Deleted: .

Yangyang 4/6/2015 1:01 PM

Deleted: . &

Yangyang 4/6/2015 1:01 PM

Deleted: .

Yangyang 4/6/2015 1:01 PM

Deleted: .

Yangyang 4/6/2015 1:01 PM

Deleted: .

Yangyang 4/6/2015 1:01 PM

Deleted: .

398 Friedman, A. R., Hwang, Y.-T., Chiang, J. C. H., and Frierson, D. M. W.: Interhemispheric
 399 temperature asymmetry over the 20th century and in future projections, *J. Clim.*, 26, 5419–5433,
 400 2013.

401 Ganguly, D., Rasch, P. J., Wang, H., and Yoon, J.: Fast and slow responses of the South Asian
 402 monsoon system to anthropogenic aerosols. *Geophys. Res. Lett.*, 39, L18804,
 403 [doi:10.1029/2012GL053043](https://doi.org/10.1029/2012GL053043), 2012.

404 Gottelman, A., Liu, X., Ghan, S. J., Morrison, H., Park, S., Conley, A. J., Klein, S. A., Boyle, J.,
 405 Mitchell, D. L. and Li, J.-L. F.: Global simulations of ice nucleation and ice supersaturation with
 406 an improved cloud scheme in the Community Atmosphere Model, *J. Geophys. Res. Atmos.*,
 407 115(D18), D18216, [doi:10.1029/2009JD013797](https://doi.org/10.1029/2009JD013797), 2010.

408 Held, I. M. and Hou, A. Y.: Nonlinear axially symmetric circulations in a nearly inviscid
 409 atmosphere, *J. Atmos. Sci.*, 37, 515–533, 1980.

410 Holton, J.: An Introduction to Dynamic Meteorology, 4th Edition, Elsevier Academic Press, San
 411 Diego, 535 pp., 2004.

412 Huang, J., Fu, Q., Zhang, W., Wang, X., Zhang, R., Ye, H., and Warren, S.: Dust and black
 413 carbon in seasonal snow across northern China, *Bull. Amer. Meteor. Soc.*, 92, 175–
 414 181, [doi:10.1175/2010BAMS3064.1](https://doi.org/10.1175/2010BAMS3064.1), 2011.

415 Hwang, Y.-T., Frierson, D. M. W., and Kang, S. M.: Anthropogenic sulfate aerosol and the
 416 southward shift of tropical precipitation in the late 20th century. *Geophys. Res. Lett.*, 40, 2845–
 417 2850, 2013.

- Yangyang 4/6/2015 1:01 PM
- Deleted: &
- Yangyang 4/6/2015 1:01 PM
- Deleted: .
- Yangyang 4/6/2015 1:01 PM
- Deleted: Temperature Asymmetry
- Yangyang 4/6/2015 1:01 PM
- Deleted: Twentieth Century
- Yangyang 4/6/2015 1:01 PM
- Deleted: Future Projections.
- Yangyang 4/6/2015 1:01 PM
- Deleted: .
- Yangyang 4/6/2015 1:01 PM
- Deleted: &
- Yangyang 4/6/2015 1:01 PM
- Deleted: .
- Yangyang 4/6/2015 1:01 PM
- Deleted: .
- Yangyang 4/6/2015 1:01 PM
- Deleted: .
- Yangyang 4/6/2015 1:01 PM
- Deleted: &
- Yangyang 4/6/2015 1:01 PM
- Deleted: .
- Yangyang 4/6/2015 1:01 PM
- Deleted: Axially Symmetric Circulations
- Yangyang 4/6/2015 1:01 PM
- Deleted: Nearly Inviscid Atmosphere.
- Yangyang 4/6/2015 1:01 PM
- Deleted: .
- Yangyang 4/6/2015 1:01 PM
- Deleted: .
- Yangyang 4/6/2015 1:01 PM
- Deleted: 1991.
- Yangyang 4/6/2015 1:01 PM
- Moved (insertion) [3]
- Yangyang 4/6/2015 1:01 PM
- Formatted: Font:Times
- Yangyang 4/6/2015 1:01 PM
- Deleted: &
- Yangyang 4/6/2015 1:01 PM
- Deleted: .
- Yangyang 4/6/2015 1:01 PM
- Deleted: .
- Yangyang 4/6/2015 1:01 PM
- Deleted: .

439 Koch, D. and Del Genio, A. D.: Black carbon semi-direct effects on cloud cover: review and
 440 synthesis. *Atmos. Chem. Phys.*, 10, 7685–7696, doi:10.5194/acp-10-7685-2010, 2010.

441 Lamarque, J.-F., Bond, T. C., Eyring, V., Granier, C., Heil, A., Klimont, Z., Lee, D., Liousse, C.,
 442 Mieville, A., Owen, B., Schultz M. G., Shindell, D., Smith, S. J., Stehfest, E., Van Aardenne, J.,
 443 Cooper, O. R., Kainuma, M., Mahowald, N., McConnell, J. R., Naik, V., Riahi, K., and van
 444 Vuuren, D. P.: Historical (1850–2000) gridded anthropogenic and biomass burning emissions of
 445 reactive gases and aerosols: methodology and application. *Atmos. Chem. Phys.*, 10, 7017–7039,
 446 doi:10.5194/acp-10-7017-2010, 2010.

447 Lau, K. M., Kim, M. K., and Kim, K. M.: Asian summer monsoon anomalies induced by aerosol
 448 direct forcing: the role of the Tibetan Plateau. *Clim. Dynam.*, 26, 855–864, 2006.

449 Levy, H., Horowitz, L. W., Schwarzkopf, M. D., Ming, Y., Golaz, J.-C., Naik, V., and
 450 Ramaswamy, V.: The roles of aerosol direct and indirect effects in past and future climate
 451 change. *J. Geophys. Res. Atmos.*, 118, 4521–4532, 2013.

452 Limpasuvan, V. and Hartmann, D.: Wave-maintained annular modes of climate variability. *J.*
 453 *Clim.*, 13, 4414–4429, 2000.

454 Liu, X., Easter, R. C., Ghan, S. J., Zaveri, R., Rasch, P., Shi, X., Lamarque, J. F., Gettelman, A.,
 455 Morrison, H., Vitt, F., Conley, A., Park, S., Neale, R., Hannay, C., Ekman, A. M. L., Hess, P.,
 456 Mahowald, N., Collins, W., Iacono, M. J., Bretherton, C. S., Flanner, M. G. and Mitchell, D.:
 457 Toward a minimal representation of aerosols in climate models: Description and evaluation in
 458 the Community Atmosphere Model CAM5, *Geosci. Model Dev.*, 5, 709–739, doi:10.5194/gmd-
 459 5-709-2012, 2012.

- Yangyang 4/6/2015 1:01 PM
Deleted: &
- Yangyang 4/6/2015 1:01 PM
Deleted: .
- Yangyang 4/6/2015 1:01 PM
Deleted: .
- Yangyang 4/6/2015 1:01 PM
Deleted: .
- Yangyang 4/6/2015 1:01 PM
Deleted: .
- Yangyang 4/6/2015 1:01 PM
Deleted: Lamarque, J.-F. et al.
- Yangyang 4/6/2015 1:01 PM
Deleted: .
- Yangyang 4/6/2015 1:01 PM
Deleted: .
- Yangyang 4/6/2015 1:01 PM
Deleted: &
- Yangyang 4/6/2015 1:01 PM
Deleted: .
- Yangyang 4/6/2015 1:01 PM
Deleted: .
- Yangyang 4/6/2015 1:01 PM
Deleted: Dyn.
- Yangyang 4/6/2015 1:01 PM
Deleted: . et al.
- Yangyang 4/6/2015 1:01 PM
Deleted: .
- Yangyang 4/6/2015 1:01 PM
Deleted: .
- Yangyang 4/6/2015 1:01 PM
Deleted: &
- Yangyang 4/6/2015 1:01 PM
Deleted: .
- Yangyang 4/6/2015 1:01 PM
Deleted: Maintained Annular Modes
- Yangyang 4/6/2015 1:01 PM
Deleted: Climate Variability.
- Yangyang 4/6/2015 1:01 PM
Deleted: .
- Yangyang 4/6/2015 1:01 PM
Moved (insertion) [4]

480 [Long, S.-M., Xie, S.-P., Zheng, X.-T. and Liu, Q.: Fast and Slow Responses to Global Warming:](#)
481 [Sea Surface Temperature and Precipitation Patterns, J. Clim., 27\(1\), 285–299, doi:10.1175/JCLI-](#)
482 [D-13-00297.1, 2013.](#)

483 [Lu, J., Chen, G. and Frierson, D. M. W.: Response of the Zonal Mean Atmospheric Circulation](#)
484 [to El Niño versus Global Warming, J. Clim., 21\(22\), 5835–5851, doi:10.1175/2008JCLI2200.1,](#)
485 [2008.](#)

486 [Manabe, S. and Wetherald, R. T.: The effects of doubling the CO2 concentration on the climate](#)
487 [of a general circulation model, J. Atmos. Sci., 32, 3–15, 1975.](#)

Yangyang 4/6/2015 1:01 PM
Deleted: &...nd Wetherald, R. T....: ... [1]

488 [Meehl, G. A., Arblaster, J. M., and Collins, W. D.: Effects of black carbon aerosols on the Indian](#)
489 [Monsoon, J. Clim., 21, 2869–2882, 2008.](#)

Yangyang 4/6/2015 1:01 PM
Moved (insertion) [5]
Yangyang 4/6/2015 1:01 PM
Deleted: Meehl,

490 [Meehl, G. A., Washington, W. M., Arblaster, J. M., Hu, A., Teng, H., Kay, J. E., Gettelman, A.,](#)
491 [Lawrence, D. M., Sanderson, B. M., and Strand, W. G.: Climate Change Projections, in](#)
492 [CESM1\(CAM5\) Compared to CCSM4, J. Clim., 26, 6287–6308, 2013.](#)

Yangyang 4/6/2015 1:01 PM
Moved up [4]: G.
Yangyang 4/6/2015 1:01 PM
Deleted: A. et al. Climate change ... [2]

493 [Ocko, I. B., Ramaswamy, V., and Ming, Y.: Contrasting climate responses to the scattering and](#)
494 [absorbing features of anthropogenic aerosol forcings, J. Clim., 27, 5329–5345, 2014.](#)

Yangyang 4/6/2015 1:01 PM
Moved up [5]: Meehl, G. A., Arblaster, J. M

495 [Painter, T. H., Flanner, M. G., Kaser, G., Marzeion, B., VanCuren, R. A., and Abdalati, W.: End](#)
496 [of the Little Ice Age in the Alps forced by industrial black carbon, P. Natl. Acad. Sci., 110,](#)
497 [15216–15221, 2013.](#)

Yangyang 4/6/2015 1:01 PM
Deleted: . & Collins, W. D. Effects of Black Carbon Aerosols on the Indian Monsoon. J. Clim. 21, 2869–2882, 2008. [3]
Yangyang 4/6/2015 1:01 PM
Deleted: H. et al....., Flanner, M. G., ... [4]

540 Ramanathan, V. and Feng, Y.: On avoiding dangerous anthropogenic interference with the
541 climate system: formidable challenges ahead, Proc. Natl. Acad. Sci. USA, 105, 14245–14250,
542 2008.

543 Ramanathan, V., Chung, C., Kim, D., Bettge, T., Buja, L., Kiehl, J. T., Washington, W. M., Fu,
544 Q., Sikka, D. R., and Wild, M.: Atmospheric brown clouds: Impacts on South Asian climate and
545 hydrological cycle, P. Natl. Acad. Sci. USA, 102, 5326–5333, 2005.

546 Rosenfeld, D., Wood, R., Donner, L., and Sherwood, S.: Aerosol Cloud-Mediated Radiative
547 Forcing: Highly Uncertain and Opposite Effects from Shallow and Deep Clouds, in: Climate
548 Science for Serving Society, edited by: Asrar, G. R. and Hurrell, J. W., 105–149, Springer
549 Netherlands, 2013.

550 Rotstajn, L. D., Plymin, E. L., Collier, M. A., Boucher, O., Dufresne, J.-L., Luo, J.-J., von
551 Salzen, K., Jeffrey, S. J., Foujols, M.-A., Ming, Y., and Horowitz, L. W.: Declining Aerosols in
552 CMIP5 Projections: Effects on Atmospheric Temperature Structure and Midlatitude Jets, J.
553 Clim., 27, 6960–6977, 2014.

554 Santer, B. D., Painter, J. F., Mears, C. A., Doutriaux, C., Caldwell, P., Arblaster, J. M.,
555 CameronSmith, P. J., Gillett, N. P., Gleckler, P. J., Lanzante, J., Perlwitz, J., Solomon, S., Stott,
556 P. a., Taylor, K. E., Terray, L., Thorne, P. W., Wehner, M. F., Wentz, F. J., Wigley, T. M. L.,
557 Wilcox, L. J., and Zou, C.-Z.: Identifying human influences on atmospheric temperature, P. Natl.
558 Acad. Sci. 110, 26–33, 2013.

559 Shindell, D. T., Voulgarakis, A., Faluvegi, G., and Milly, G.: Precipitation response to regional
560 radiative forcing, Atmos. Chem. Phys., 12, 6969–6982, doi:10.5194/acp-12-6969-2012, 2012.

- Yangyang 4/6/2015 1:01 PM
Deleted: &
- Yangyang 4/6/2015 1:01 PM
Deleted: .
- Yangyang 4/6/2015 1:01 PM
Deleted: .
- Yangyang 4/6/2015 1:01 PM
Deleted: U. S. A.
- Yangyang 4/6/2015 1:01 PM
Deleted: 50
- Yangyang 4/6/2015 1:01 PM
Deleted: . et al.
- Yangyang 4/6/2015 1:01 PM
Deleted: impacts
- Yangyang 4/6/2015 1:01 PM
Deleted: . Proc
- Yangyang 4/6/2015 1:01 PM
Deleted: U. S. A.
- Yangyang 4/6/2015 1:01 PM
Deleted: 33
- Yangyang 4/6/2015 1:01 PM
Moved (insertion) [6]
- Yangyang 4/6/2015 1:01 PM
Deleted: Rosenfeld, D. & Wood, R. Aerosol cloud-mediated radiative forcing: highly uncertain and opposite effects from shallow and deep clouds. Clim. Sci. Serv
- Yangyang 4/6/2015 1:01 PM
Moved up [3]: . Soc.,
- Yangyang 4/6/2015 1:01 PM
Moved up [6]: Rotstajn, L. D
- Yangyang 4/6/2015 1:01 PM
Formatted: Font:Times
- Yangyang 4/6/2015 1:01 PM
Deleted: 2013. .
- Yangyang 4/6/2015 1:01 PM
Deleted: . et al.
- Yangyang 4/6/2015 1:01 PM
Deleted: .
- Yangyang 4/6/2015 1:01 PM
Deleted: .
- Yangyang 4/6/2015 1:01 PM
Deleted: . et al.
- Yangyang 4/6/2015 1:01 PM
Deleted: . Proc
- Yangyang 4/6/2015 1:01 PM
Deleted: .
- Yangyang 4/6/2015 1:01 PM
Deleted: -

585 Smith, S. J., van Aardenne, J., Klimont, Z., Andres, R. J., Volke, A., and Delgado Arias, S.:
586 Anthropogenic sulfur dioxide emissions: 1850–2005. *Atmos. Chem. Phys.*, 11, 1101–1116, 10
587 doi:10.5194/acp-11-1101-2011, 2011.

Yangyang 4/6/2015 1:01 PM

Deleted: . et al...., van Aardenne, J., ... [5]

588 Sun, L., Chen, G., and Lu, J.: Sensitivities and mechanisms of the zonal mean atmospheric
589 circulation response to tropical warming. *J. Atmos. Sci.*, 70, 2487–2504, 2013.

Yangyang 4/6/2015 1:01 PM

Deleted: . &..., and Lu, J....: Sensitiv ... [6]

590 Vиноj, V., Rasch, P. J., Wang, H., Yoon, J.-H., Ma, P.-L., Landu, K., and Singh, B.: Short-term
591 modulation of Indian summer monsoon rainfall by West Asian dust. *Nat. Geosci.*, 7, 308–313,
592 2014.

Yangyang 4/6/2015 1:01 PM

Deleted: . et al...., Rasch, P. J., Wang ... [7]

593 Xie, S.-P., Deser, C., Vecchi, G. A., Ma, J., Teng, H. and Wittenberg, A. T.: Global Warming
594 Pattern Formation: Sea Surface Temperature and Rainfall, *J. Clim.*, 23, 966–986,
595 doi:10.1175/2009JCLI3329.1, 2010.

596 Xie, S., Lu, B., and Xiang, B.: Similar spatial patterns of climate responses to aerosol and
597 greenhouse gas changes. *Nat. Geosci.*, 6, 828–832, 2013.

Yangyang 4/6/2015 1:01 PM

Deleted: . &..., and Xiang, B....: Sim ... [8]

598 Xu, Y. and Ramanathan, V.: Latitudinally asymmetric response of global surface temperature:
599 implications for regional climate change. *Geophys. Res. Lett.*, 39, L13706,
600 doi:10.1029/2012GL052116, 2012.

Yangyang 4/6/2015 1:01 PM

Deleted: &...nd Ramanathan, V....: ... [9]

601 Xu, Y., Bahadur, R., Zhao, C., and Ruby Leung, L.: Estimating the radiative forcing of
602 carbonaceous aerosols over California based on satellite and ground observations. *J. Geophys.*
603 *Res.-Atmos.*, 118, 11148–11160, 2013.

Yangyang 4/6/2015 1:01 PM

Deleted: . &..., and Ruby Leung, L.... [10]

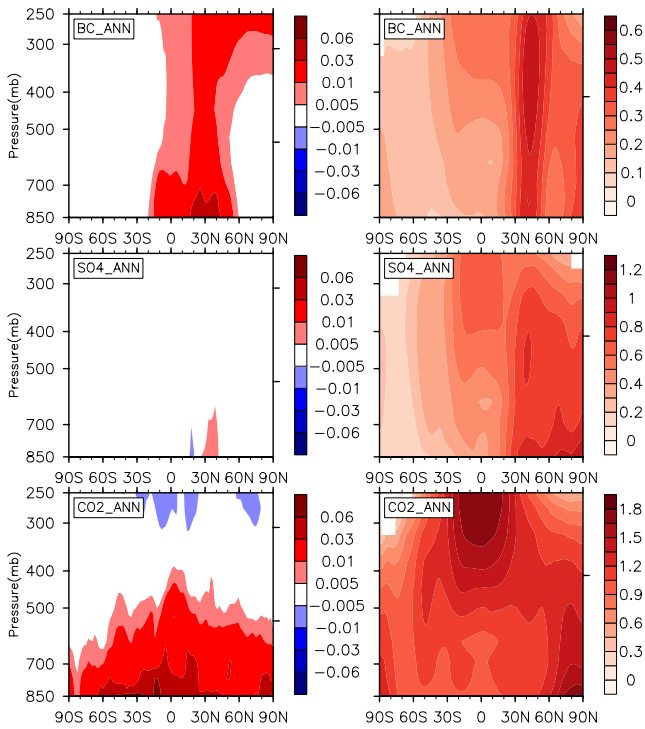
Yangyang 4/6/2015 1:01 PM

Formatted: Font:12 pt

Yangyang 4/6/2015 1:01 PM

Formatted: Line spacing: double

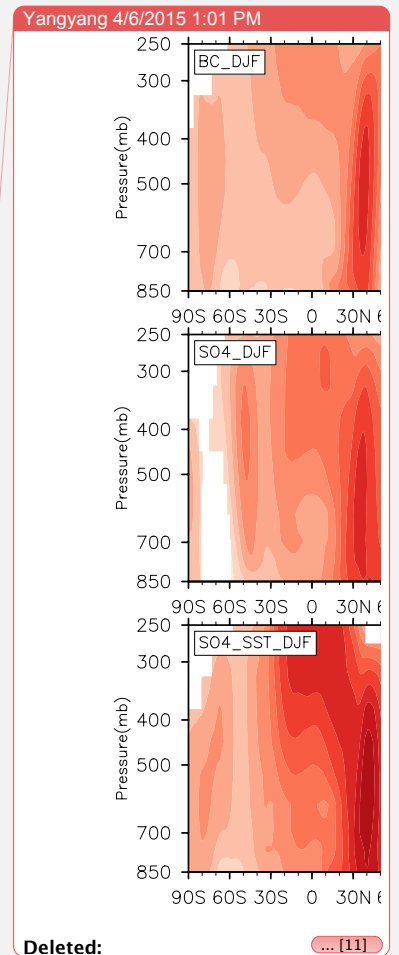
639 Figures:

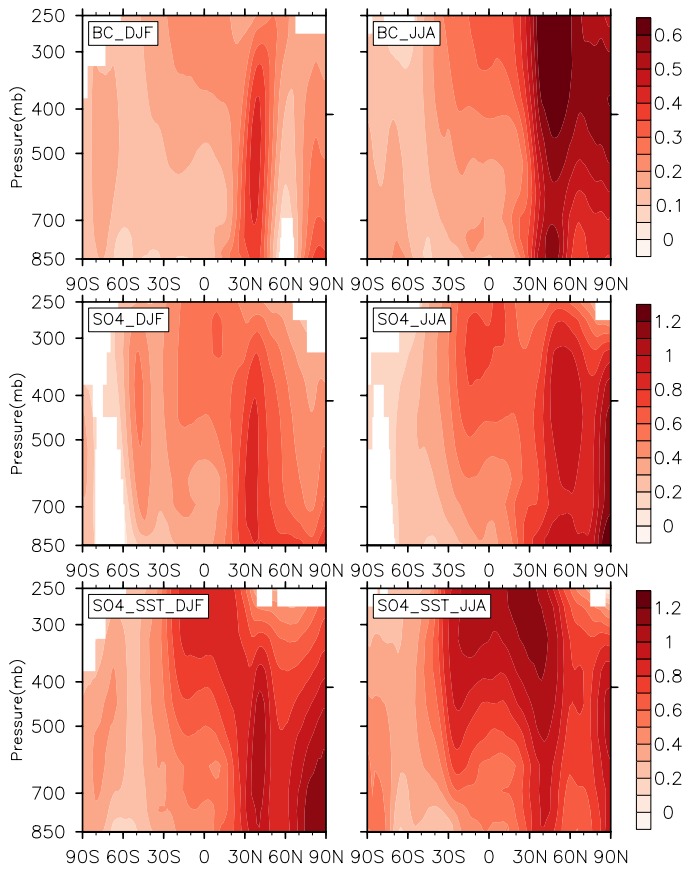


640

641 Fig. 1: (Left) Heating rate ($^{\circ}\text{C}/\text{day}$) due to increase of BC, SO₄ and CO₂ atmospheric
642 concentration. The heating rate is diagnosed by contrasting two sets of five-year atmospheric-
643 only simulations with pre-industrial and present-day emissions/concentrations, respectively.
644 (Right) Annually averaged atmospheric temperature in response due to the forcing of BC, SO₄
645 and CO₂. The color scale for SO₄ is reversed. The magnitude of color scale is chosen
646 considering the difference in top-of-atmosphere forcing (Table S1).

647





651

652 **Fig. 2: Temperature response (°C)** as a function of latitude and pressure to BC (1st row), SO4
 653 (2nd row), and SO4-induced SST perturbation (SO4_SST) (3rd row). The left and right columns
 654 are the DJF and JJA average, respectively. Note that the color scales for SO4 and SO4_SST are
 655 reversed.

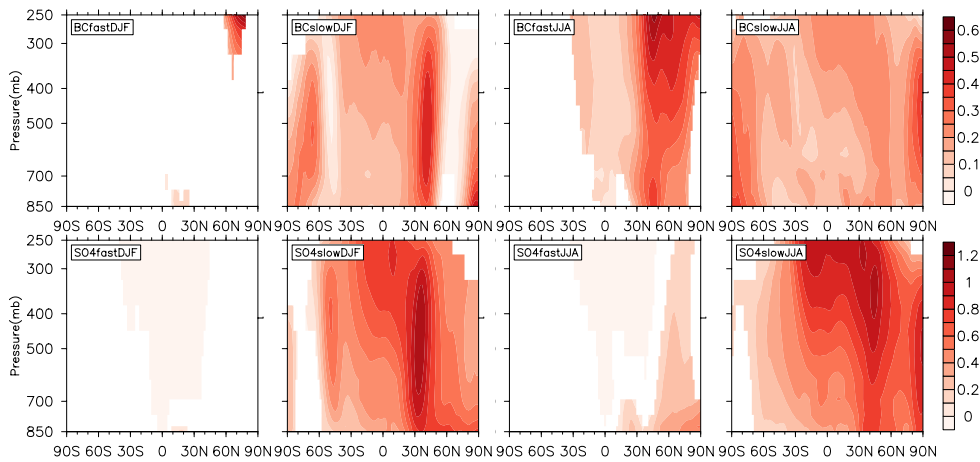
656

Yangyang 4/6/2015 1:01 PM
Formatted: Left, Space Before: 6 pt, After: 0 pt

Yangyang 4/6/2015 1:01 PM
Deleted: Note that the SO4 and SO4_SST response are of the opposite sign. The color scale is chosen considering that the top-of-atmosphere forcing of SO4 is about twice that of BC in this model.

Yangyang 4/6/2015 1:01 PM
Deleted: [Page Break](#)

Yangyang 4/6/2015 1:01 PM
Deleted: -

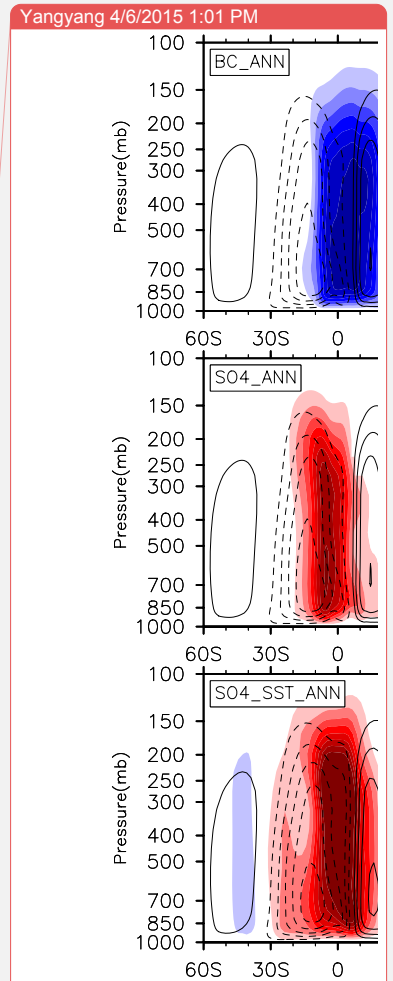
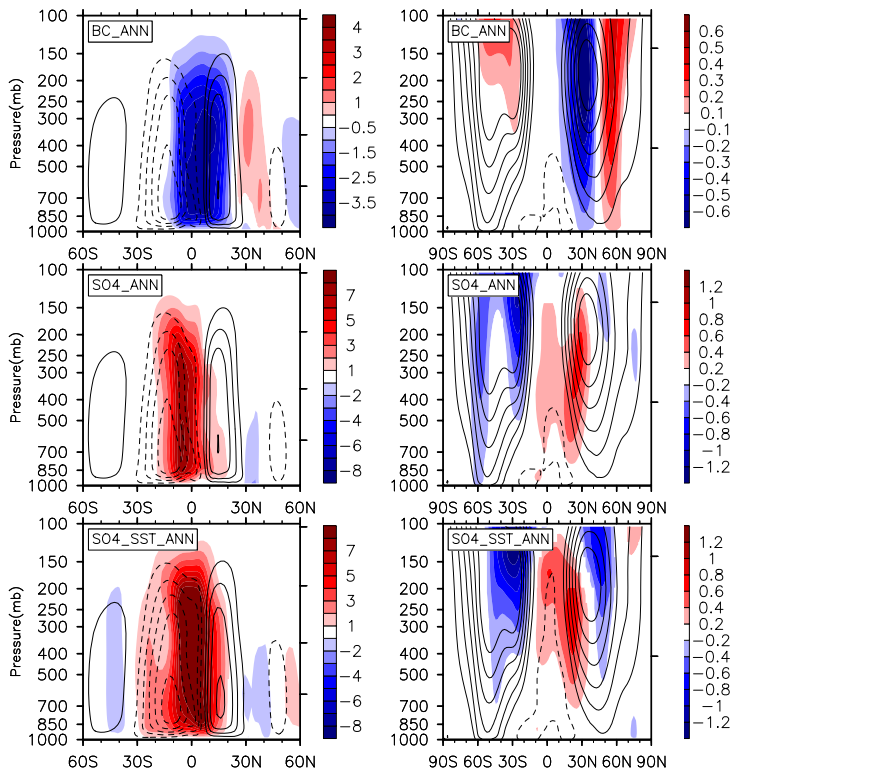


664

665 Fig. 3: Similar to Fig. 2, but for fast (1st and 3rd column) and slow components (2nd and 4th
 666 column) of temperature response (in °C). The fast component is calculated by running the
 667 atmospheric-only (fixed SST) simulation with perturbed atmospheric compositions, while the
 668 slow component is the difference between the total (Fig. 2) and fast component. The color scale
 669 for SO4 is reversed.

670

- Yangyang 4/6/2015 1:01 PM
Formatted: Left, Space Before: 6 pt, After: 0 pt
- Yangyang 4/6/2015 1:01 PM
Deleted: 2
- Yangyang 4/6/2015 1:01 PM
Deleted: Figure 1
- Yangyang 4/6/2015 1:01 PM
Deleted: K
- Yangyang 4/6/2015 1:01 PM
Deleted: an
- Yangyang 4/6/2015 1:01 PM
Deleted: changed
- Yangyang 4/6/2015 1:01 PM
Deleted: but fixed SST,
- Yangyang 4/6/2015 1:01 PM
Deleted: 1
- Yangyang 4/6/2015 1:01 PM
Deleted: responses

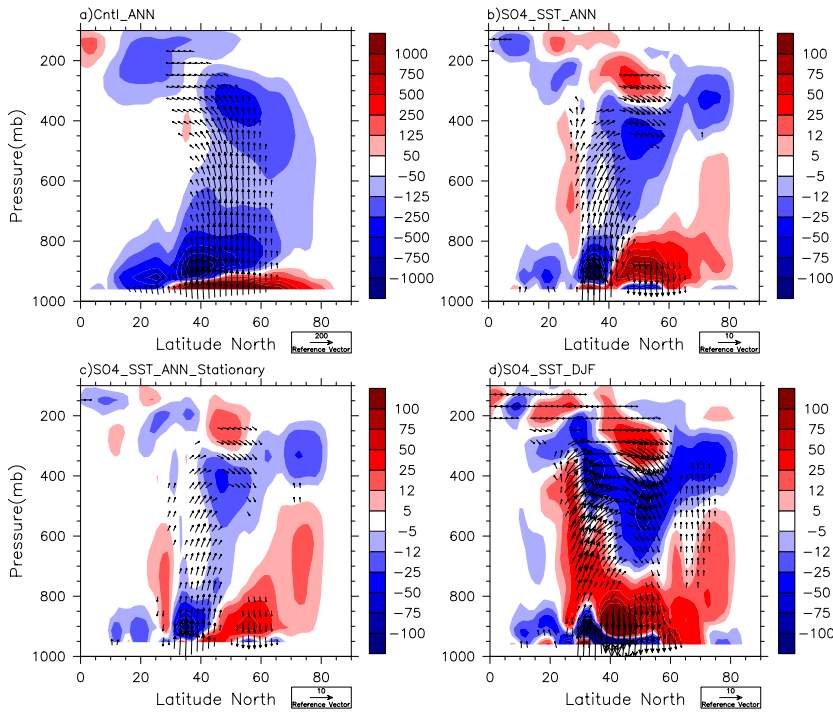


Deleted:
 Yangyang 4/6/2015 1:01 PM
 Deleted: 3:

Yangyang 4/6/2015 1:01 PM
 Moved (insertion) [7]

Yangyang 4/6/2015 1:01 PM
 Formatted

679
 680 Fig. 4: (left) Zonal mean meridional stream function change (10^9 kg/s), in response to BC (1st
 681 row), SO₄ (2nd row), and SO₄-induced SST perturbation (SO₄_SST) (3rd row). Climatological
 682 stream function is shown in contour lines with an interval of 40. The negative values (blue
 683 shading and dashed lines) of the stream function indicate that the meridional flow is counter-
 684 clockwise. (right) Zonal mean zonal wind (U) change under various cases. The climatological jet
 685 stream is around 30°N to 60°N at 250 mb (line contours). Under SO₄ forcing, the NH jet stream
 686 shifts significantly equatorward.
 687



Yangyang 4/6/2015 1:01 PM

Deleted:
 Unknown
Formatted: Kern at 14 pt
 Unknown
Formatted: Kern at 14 pt

690

691 Fig. 5: The Eliassen-Palm (EP) flux (vector) and its divergence (contour). (a) The climatology.
 692 (b) The change due to SO₄-induced SST perturbation (SO₄_SST). The convergence (blue) and
 693 divergence (red) of the EP flux correspond to a deceleration and acceleration of the westerly
 694 mean flow, respectively. (c) Contributions of the stationary eddy to the change shown in (b).
 695 This was calculated using 10-day average, instead of daily average. Transient eddies are the
 696 difference between the total and stationary contribution (not shown). (d) NH winter (DJF)
 697 average, not the annual average shown (b). Note the color scale and reference vectors are
 698 different across the panels.

Yangyang 4/6/2015 1:01 PM
Formatted: Acknowledgement, Justified, Space Before: Auto, After: Auto, Line spacing: double
 Yangyang 4/6/2015 1:01 PM
Deleted: 4:
 Yangyang 4/6/2015 1:01 PM
Formatted
 Yangyang 4/6/2015 1:01 PM
Deleted: solid contours
 Yangyang 4/6/2015 1:01 PM
Deleted: dashed contours
 Yangyang 4/6/2015 1:01 PM
Moved (insertion) [8]
 Yangyang 4/6/2015 1:01 PM
Deleted: .

704 **Supplement materials for**

705 **Ocean mediation of tropospheric response to reflecting and absorbing aerosols**

706

707 Yangyang Xu^{1*} and Shang-Ping Xie²

708

709 ¹National Center for Atmospheric Research, Boulder, CO 80303.

710 ²Scripps Institution of Oceanography, University of California, San Diego, La Jolla, CA 92093.

711 *Correspondence to: yangyang@ucar.edu

712

Yangyang 4/6/2015 1:01 PM
Formatted: Font:12 pt

Yangyang 4/6/2015 1:01 PM
Deleted: -

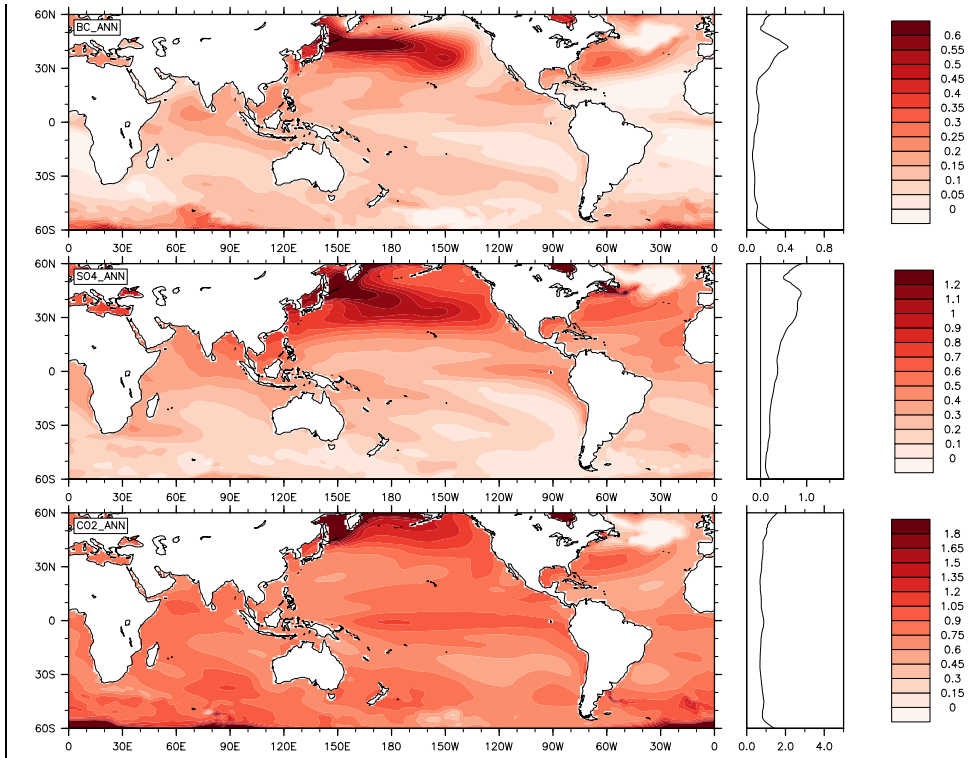
Yangyang 4/6/2015 1:01 PM
Formatted: Font:12 pt

714 Table S1. (a) TOA forcing (W/m^2 , shortwave and longwave) due to BC (direct radiative forcing
 715 from pre-industrial to present-day; not including snow albedo effect), SO4 (direct and indirect
 716 forcing from pre-industrial to present-day, so called “adjusted forcing”) and CO2 (from pre-
 717 industrial to present-day at 400 ppm). The radiative forcing is diagnosed by contrasting two sets
 718 of five-year atmospheric-only simulations with pre-industrial and present-day
 719 emissions/concentrations, respectively. (b) Surface temperature change ($^{\circ}C$) in response to
 720 different forcings in (a). These are calculated from the 60-year average of coupled model
 721 simulation. (c) Cumulative precipitation (cm) change in response to different forcings in (a). The
 722 relative changes in percentage are shown in parenthesis next to the absolute changes.
 723

	BC	SO4	CO2
(a) TOA net forcing (W/m^2)	0.5	-0.9	1.7
(b) Surface temperature change ($^{\circ}C$)	0.21	-0.49	1.15
(c) Cumulative precipitation (cm)	-0.01 (0%)	-2.09 (-2%)	1.73 (2%)

724

- Yangyang 4/6/2015 1:01 PM
Formatted: Superscript
- Yangyang 4/6/2015 1:01 PM
Deleted: +
- Yangyang 4/6/2015 1:01 PM
Deleted: ,
- Yangyang 4/6/2015 1:01 PM
Deleted: +
- Yangyang 4/6/2015 1:01 PM
Deleted: effect
- Yangyang 4/6/2015 1:01 PM
Deleted: ”,
- Yangyang 4/6/2015 1:01 PM
Deleted:) and CO2 (pre-industrial to
- Yangyang 4/6/2015 1:01 PM
Deleted: calculated
- Yangyang 4/6/2015 1:01 PM
Deleted: running
- Yangyang 4/6/2015 1:01 PM
Deleted: model for 5 years (same as Fig S1a).
- Yangyang 4/6/2015 1:01 PM
Deleted: Surface temperature change is
- Yangyang 4/6/2015 1:01 PM
Deleted: a
- Yangyang 4/6/2015 1:01 PM
Deleted: forcing agents.
- Yangyang 4/6/2015 1:01 PM
Deleted: change of cumulative precipitation
- Yangyang 4/6/2015 1:01 PM
Deleted: is
- Yangyang 4/6/2015 1:01 PM
Deleted: change
- Yangyang 4/6/2015 1:01 PM
Formatted: Superscript



Yangyang 4/6/2015 1:01 PM

Deleted: ... [12]

Unknown

Formatted: Font:12 pt

741

742 Fig. S1: Sea Surface temperature change (°C) change in response to BC, SO4 and CO2 forcings.

743 These are calculated from the 60-year average of coupled model simulation. Color scale for SO4
 744 is reversed.

745

746

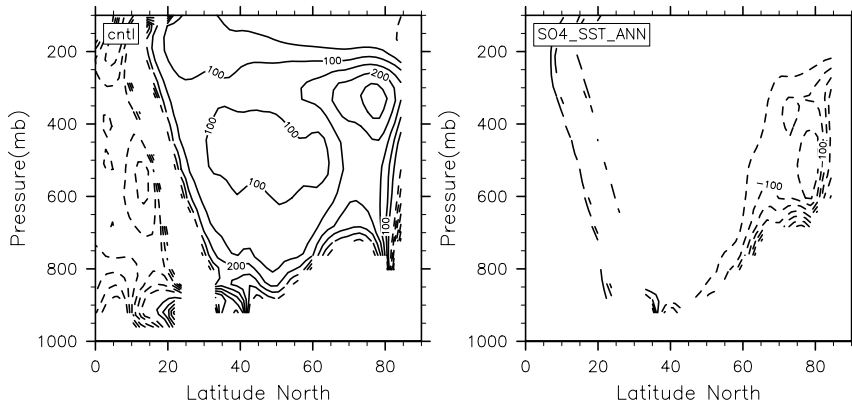


Fig. S2: Refractive index in the climatology (left panel) and its change due to SO4-induced SST perturbation (right panel). The contour plot is limited to 0–400, following Figure 8 of Limpasuvan and Hartmann (2000), to highlight the contours in the mid-latitude regions where the wave activities are strongest.

- Yangyang 4/6/2015 1:01 PM

Moved down [9]: GHG forcing is fixed in this simulation. An ensemble of three simulations was conducted. .
- Yangyang 4/6/2015 1:01 PM

Formatted: Indent: First line: 0"
- Yangyang 4/6/2015 1:01 PM

Moved up [7]: mean zonal wind (U) change under various cases. The climatological jet stream is around 30°N to 60°N at 250 mb (line contours). Under SO4 forcing, the NH jet stream shifts significantly equatorward.
- Yangyang 4/6/2015 1:01 PM

Moved up [8]: . Transient eddies are the difference between the total and stationary contribution (not shown). (
- Yangyang 4/6/2015 1:01 PM

Deleted: —Page Break—

- ... [13]
- Yangyang 4/6/2015 1:01 PM

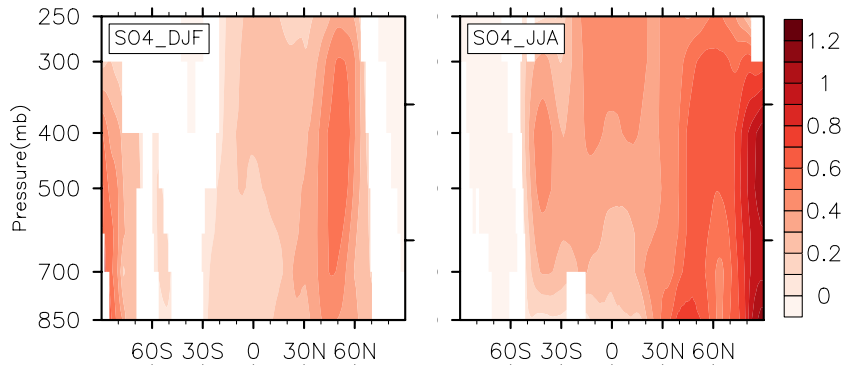
Deleted: —Page Break—

- ... [14]
- Yangyang 4/6/2015 1:01 PM

Deleted: c) shows the boreal winter (DJF) average, not the annual average that is shown in Fig 4. Note the reference vector changes across the panels (200, 10, 20). [15]

778

779



780

781

782 Fig. S3: Similar to the 2nd row of Figure 1, but showing the trend of temperature changes
783 (°C/decade) during 1940-1970 in the 20th century transient climate simulation using the same
784 model (CESM1) with time-evolving aerosol-only forcing. During this period, SO₂ emissions
785 rapidly increased. Color scale is reversed to be consistent with Fig. 1. GHG forcing is fixed in
786 this simulation. An ensemble of three simulations was conducted.

787

Yangyang 4/6/2015 1:01 PM

Formatted: Indent: First line: 0"

Yangyang 4/6/2015 1:01 PM

Moved (insertion) [9]